Single-lap joints of similar and dissimilar adherends bonded with a polyurethane adhesive used in the automotive industry

(Article begins on next page)

25 April 2024

PAPER • OPEN ACCESS

Single-lap joints of similar and dissimilar adherends bonded with a polyurethane adhesive used in the automotive industry

View the article online for updates and enhancements.

Single-lap joints of similar and dissimilar adherends bonded with a polyurethane adhesive used in the automotive industry

R Ciardiello[1,2]*, C Boursier Niutta[1], F Di Sciullo[3], L Goglio[1,2]

[1] Department of mechanical and aerospace engineering, Politecnico di Torino, Torino 10129, IT
[2] J-TECH@POLITO, Politecnico di Torino, Torino 10129, IT
[3] Group Materials Labs, Centro Ricerche Fiat, Torino 10135, IT

Email: raffaele.ciardiello@polito.it, carlo.boursier@polito.it, fiorenza.disciullo@crf.it, luca.goglio@polito.it

Abstract. The mechanical performances of single-lap joints between similar and dissimilar adherends bonded with a bi-component polyurethane adhesive have been studied in the present work. The substrate materials include both carbon fibre reinforced composite material (CRFP) and painted metal substrates (PMS). The following substrate combinations were tested: CFRP/CFRP, PMS/PMS, and CFRP/PMS. Two adhesive overlaps, 12 mm and 24 mm, with a fixed thickness were studied to assess the mechanical behaviour of the adhesive joints. The experimental results have been used to construct a finite element model of the single lap joint tests. The objective is to determine the material cohesive properties, in particular the maximum shear stress and the corresponding energy release rate, of the adhesive layer for each retained combination of substrates. An optimization scheme based on transient nonlinear finite element analysis has been here considered, where cohesive parameters of the adhesive layer are handled as design variables. Material parameters are firstly identified for the 12 mm overlap, minimizing the discrepancy between the experimental and numerical force-displacement curves. Then, to validate the obtained properties, results of the 24 mm overlap single lap joint tests are used. The comparison between the experimental and numerical results shows a very good agreement.

1. Introduction

Lightweight design strategies are widely adopted in the transportation industry. This is related to the possibility to reduce fuel consumption by reducing vehicle weight and so vehicle emissions that are subject to increasing restriction set by governments [1]. To this aim, the adoption of lightweight materials (e.g., composite materials, Al or Mg alloys) characterized by a high specific strength have been widely adopted by industry in order to reduce the vehicle weight without affecting the mechanical performance of the vehicle structures. The adoption of composite materials acquired particular relevance in the automotive industry due to the emission targets. Their adoption in the car industry has been quite challenging and, in some cases, required to change the way to assembly new vehicles. Many research works [2, 3] showed that the holes in composite materials lead to premature failure of the composite laminate or components. For this reason, the adoption of the traditional mechanical fasteners (e.g.,

screws, bolts, rivets, etc.) cannot be easily adopted with composite materials. Composite materials are usually adhesively bonded to metal structures or other composite materials since it was demonstrated that they exhibit a better stress distribution compared to the traditional fasteners [4, 5]. Furthermore, they are usually preferred to traditional fasteners when joining components made of different materials [6, 7].

In the last years, the use of polyurethane adhesive, which is a ductile adhesive, spread in the automotive industry due to its capacity to sustain larger deformations [8] and resist to dynamic load [8-10]. Furthermore, their relatively high viscosity can be used to cover and bonds also components that present relatively large clearances. The mechanical behaviour of single lap joints by using the same adherends has been widely investigated whereas there is limited literature for adhesive joints with dissimilar materials, especially for polyurethane adhesives. In this work, the mechanical behaviour of adhesive joints made with a bi-component polyurethane adhesive has been assessed by using single lap joint (SLJ) tests. The experimental activity was carried out on painted metal steel substrate (PMS) and carbon fibre reinforced composite (CFRC) used in the automotive industry. There are few works in the literature [10-12] on the mechanical properties of polyurethane adhesives which used metal substrates only treated with primers or heat treatments and standard composite substrates (twill layers or unidirectional) [13, 14]. However, these adhesives are often used in the industry to bond painted substrate and composite materials that are constituted by different layers that present different mechanical properties and different areal weight. The activity presented in this paper has been performed by using painted steel and composite substrate properly designed for the automotive industry. The composite substrates are made of four different layers and present a higher areal weight in correspondence of the bonding area. By contrast, the layer on the other side presents the lowest areal weight since this can ease the painting process. The use of these substrates makes this work, to the authors' knowledge, new for the literature since there are no other works that use these substrates in combination with polyurethane adhesive.

The experimental results have been used to construct a numerical model of the single-lap joint test. In particular, the objective is to determine the material cohesive properties, i.e. the maximum shear stress and the corresponding energy release rate, of the adhesive layer for each considered combination of substrates. The maximum peel component is assumed equal to the double of the maximum shear stress, while the critical strain energy release rate of mode I is proportional to that of mode II as calculated by Banea et al. [10] and Leal et al. [12]. Transient nonlinear finite element analysis has been performed to simulate the mechanical behaviour of the single lap joint test of the polyurethane adhesive. An optimization scheme has been adopted, where the cohesive parameters of the adhesive layer to be identified are handled as design variables. In particular, for each retained combination of substrates, the discrepancy between the experimental and numerical load-displacement curves for the 12 mm overlap is minimized. Then, to validate the optimized parameters, the experimental results of the 24 mm overlap tests are considered. The very good agreement in terms of both absorbed energy and maximum force for all the combinations of substrates validated the material model, thus enabling to investigate the mechanical behavior of different overlaps. Furthermore, the numerical model allows to investigate with reduced time and cost different aspects such as those related to the manufacturing process in automotive applications.

2. Materials and methods

The description of the adopted materials and methods are presented in this Section.

2.1 Materials
Painted metal substrates and carbon reinforced composite materials have been used for the experimental activity. The metal substrates are made of steel (DD11) and are typically used for the cold forming process in the automotive industry. The substrates used for the experimental tests were strips 100 mm

long with cross-section 20 mm × 2.2 mm. These substrates present an ultimate tensile strength of 240 MPa, Young's modulus of 207 MPa, and a maximum elongation of 24%. The substrates were painted using a cataphoresis process adopted in the automotive industries.

The composite substrates used for the test activity are made of four different twill 2 × 2 types. The composite plate is constituted by four layers that present the following stacking sequence: GG204T, GG180P, GG204T, and GG630T supplied by Impregnatex Compositi (Italy). The composite materials were laminated in SPARCO (Italy). The layer in contact with adhesive, GG630T, presents the highest areal weight, 630 gsm, and the highest thickness of 0.65 mm. The mechanical behaviour of this composite laminate is given by the stiffer layer and it presents a tensile strength of 730 MPa, Young's modulus of 60 MPa, and a maximum elongation along 0° of 1.21%. The layers GG204T and GG180T present an areal weight that is respectively 204 and 180 gsm and both have a thickness of 0.25 mm. This stacking sequence is adopted for many composite components adopted in the automotive industry (e.g. roof, bonnet, and aesthetical components) since the lower thickness of the external layer can facilitate the painting process. The composite substrates were 100 mm long with cross-section 20 mm × 1.3 mm.

The substrates were bonded with a bi-component polyurethane adhesive, Betaforce 2850L by Du Pont (United States). This adhesive presents a maximum tensile strength of 8.2 MPa, Young's modulus of 20 MPa, and a maximum elongation of 114%. At least five replications were carried out for each joint configuration. All the SLJ tests were performed at a speed of 2 mm/min. Both similar and dissimilar SLJ were tested with the following substrate combinations: CFRP/CFRP, PMS/PMS, and CFRP/PMS.

2.2 Mechanical model

The mechanical behavior of the single lap joints with overlaps of 12 mm and 24 mm has been simulated for each combination of substrates with a transient nonlinear finite element analysis in LS-Dyna environment. The adherends are modeled with four-nodes shell elements while the adhesive with eight-nodes solid elements. In particular, the Belytshcko-Tsai shell elements with one integration point in the element plane are used for the adherends. Three integration points through the thickness are considered for the painted steel substrates, while the CFRP substrates have four integration points through the thickness in accordance with the number of layers. In regards to the adhesive elements, a specific cohesive formulation has been considered which assumes four integration points, located on the mid-surface of the solid element.

A 2 mm mesh size has been adopted for the adherends in the region far from the adhesive. In proximity to the overlap zone, the mesh of adherends and adhesive has been refined to the mean value of 1 mm. The numerical model of the SLJ with 12 mm of overlap is shown in Figure 1a. The same mesh size has been used for all the joint configurations.

The single-lap joint test is simulated by clamping the extremity of one adherend and applying a prescribed motion law to the other. The motion is applied through a velocity-time law which is characterized by an initial ramp then followed by a constant value of the velocity as done in [15].

Since the substrates remain in elastic field during the SLJ experimental tests, the material of painted steel adherends is modeled as perfectly elastic. In regards to the CFRP substrates, an orthotropic material model is considered for each fabric.

The nonlinearities of the single lap joint test generally cause a mixed-mode failure of the adhesive. Indeed, the small misalignments and rotations lead to the presence of both shear and peel stresses. For this reason, the adhesive material formulation takes into account the interaction between fracture modes I and II. In particular, *MAT_GENERAL_COHESIVE has been selected [16], which considers an irreversible loading/unloading path. This material model is strain rate independent [16]. This model presents a user defined traction-separation law. Further, the velocity that has been imposed at the nodes of one adherend was set through a specific curve in Ls-Dyna. The curve presents an increasing and gradual trend of the velocity. In particular, the curve presents a trend that is horizontal tangent in the first instant and then it increases with a sinusoidal trend. After this point, the curve increases with a constant trend. Before reaching the constant final value, the trend is again sinusoidal, in order to reach the constant value in a gradual way. These gradual approaches in the initial part of the curve and in the

proximity of the constant final value allows for limiting the dynamic effect. In particular, the peel and shear tractions and the corresponding energy release rates are combined with user defined points, thus defining the mechanical behaviour of the material. The shear stress and the critical strain energy release rate of mode II are handled as design variables of the structural mechanical problem described in the next section. In this paper, we considered 6 points from the normalized load-displacement curves of the experimental test of the 12 mm overlap joints. In particular, the 6 points are assumed as follows: the first corresponds to the origin, the second is considered in correspondence of the 20% of the maximum load, the third in correspondence of the 80% of the maximum load, the fourth in correspondence of the maximum load, the fifth when the load drops to the 50% of the maximum value and, finally, the last point corresponds to the maximum displacement. The generic material model is shown in Figure 1b, while Figure 1c reports the 6 points considered for the normalized load-displacement curve.
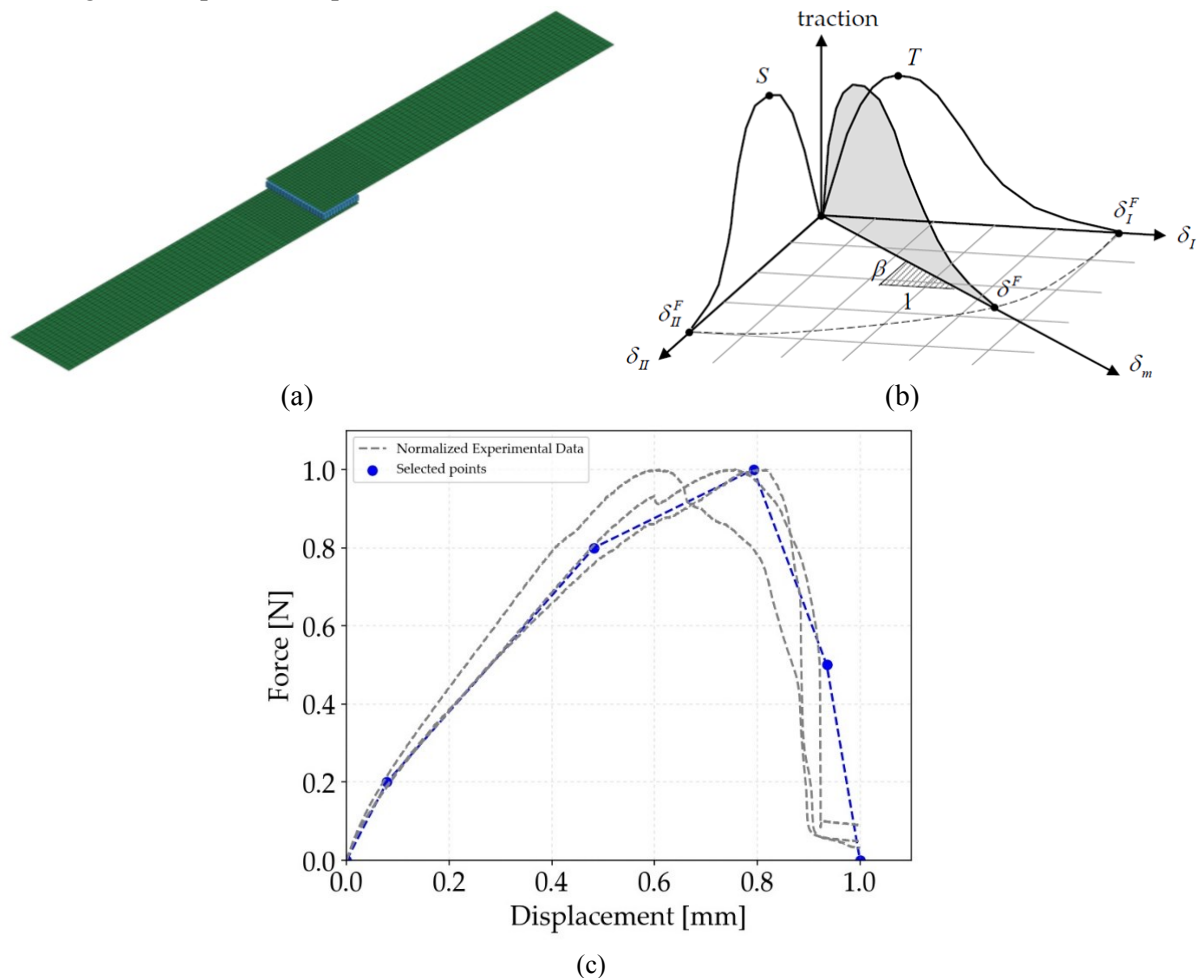

(a)   (b)

(c)

Figure 1. (a) numerical model of the single lap joint with 12 mm of overlap; (b) LS-Dyna material model; (c) 6 points considered for the normalized load-displacement curve

2.3 Structural mechanical problem

For each combination of the substrates, experimental results of the single lap joint test of the 12 mm overlaps have been used to set the material behavior. Only two material parameters have been considered to approximate the mechanical behavior of each joint. These are the shear stress S and the critical strain energy release rate of mode II G_{IIC}. In regards to the peel stress T and the corresponding energy release rate G_{IC}, these have been correlated to the design variables as follows. The maximum peel component T is assumed equal to the double of the maximum shear stress, in accordance with the Tresca criterion.

For the critical strain energy release rate of mode I, we considered the experimental results reported by Banea et al. [10] et Leal et al. [12], which refer to a polyurethane adhesive. From these, it can be assumed that G_{IC} is equal to one quarter of G_{IIC}.

In order to replicate the mechanical behavior of the single lap joint tests with 12 mm of overlaps, a surrogate model-based optimization has been carried out, which minimizes the difference between the energy absorbed by the joint in the experimental test and the numerical simulation. As the optimization is repeated for each combination of the substrates, the surrogate model-based approach allowed to reduce the computational effort. In order to properly describe the mechanical behavior of the joints, the maximum forces are constrained by the corresponding experimental values. The absorbed energy and the maximum force are surrogated using the Kriging [17] approximating method. In order to construct the surrogating surfaces, in addition to 4 corner samples, we considered 30 samples stochastically disposed in the design domain. Tables 1, 2 and 3 report the design domain limits for the PMS/PMS substrates, the CFRP/CFRP substrates and the PMS/CFRP substrates. The optimization problem is formulated as follows:

$$\min_{x \in X} f(x)$$

$$\text{such that } g_1 = \frac{F_{\max,num}(x)}{F_{\max,exp}} - 1 \le 0 \tag{1}$$

$$\text{where} \quad f = \left| EN_{num} - EN_{exp} \right|$$

$$x = \left[S, G_{IIC} \right]$$

where EN and F_{max} are respectively the absorbed energy (area under the load-displacement curve) and the maximum force.

The experimental results in terms of absorbed energy and maximum force are reported in Table X for each combination of the substrates.

Table 1. Upper and lower bounds for the single lap joint with PMS/PMS substrates

	Lower bound	Upper bound	Unit
S	8.0	13.0	MPa
G_{IIC}	16.0	26.0	N/mm

Table 2. Upper and lower bounds for the single lap joint with CFRP/CFRP substrates

	Lower bound	Upper bound	Unit
S	5.0	11.0	MPa
G_{IIC}	10.0	22.0	N/mm

Table 3. Upper and lower bounds for the single lap joint with PMS/CFRP substrates

	Lower bound	Upper bound	Unit
S	5.5	11.5	MPa
G_{IIC}	10.0	22.0	N/mm

3. Results and discussion
In this Section, the mechanical tests are reported and discussed

3.1 Experimental tests

The load-displacement curves are reported in Figures 2a, b and c. The curves related to the SLJ tests prepared with similar and dissimilar substrates, PMS, CRFP, and CRFP-PMS, are reported in Figures 2a, b and c respectively. The curves reported in this section are representative of the mechanical behaviour of the SLJ specimens. Figures 2a, b and c show that the SLJ prepared with PMS-PMS substrates exhibit the highest maximum loads for both the adhesive joints prepared with the overlap of 12 and 24 mm. On the other hand, the joints prepared with composite substrates present the lowest values of the maximum load. Figure 2c shows the load-displacement curves of the SLJ prepared with PMS and CRFP substrate for the two different overlaps. It is noticeable that the adhesive joints PMS-CRFP presents intermediate loads compared to the PMS-PMS and CRFP-CRFP specimens. This behaviour has been assessed by Reis et al. [18] on epoxy adhesives. They found that this behaviour is a direct consequence of the rigidity of the adherents that, when is higher, led to a higher failure load. Another interesting aspect of the Figures 2a, b and c, is that there is no significant difference in the maximum displacement for the SLJ prepared with 12 and 24 mm despite the significant difference of the overlap, 12 mm.
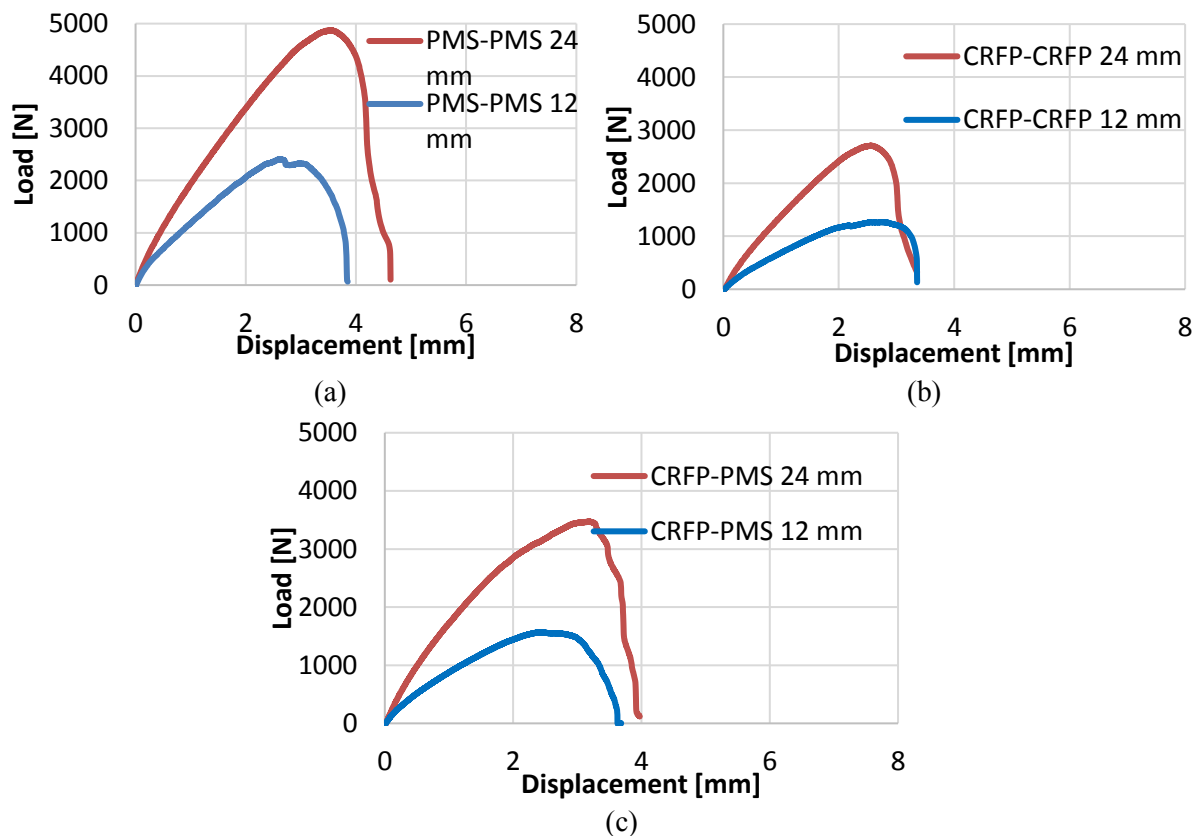

Figure 2. (a) Load - displacement curves of SLJ prepared with only PMS substrates; (b) Load - displacement curves of SLJ prepared with only CRFP substrates; (c) Load - displacement curves of SLJ prepared with only CRFP-PMS substrates

Figure 3 presents a summary of the experimental results for all the investigated joints. As shown in Figures 2a, b, and c, the joints having stiffer adherends, such as steel, present the highest shear stresses. The SLJ prepared with PMS-PMS substrates exhibited the maximum shear stress, 10.3 and 10.4 for the 12 and 24 overlaps respectively. By contrast, the SLJ prepared with CRFP-CRFP present the lowest maximum shear strengths, 5.6 MPa for both the joints, 45% lower compared to the PMS-PMS joints.

Finally, the dissimilar SLJ present intermediate maximum shear stress, that is 7.3 MPa for both the overlaps, that corresponds to a decrease of 29% compared to the PMS-PMS joints.
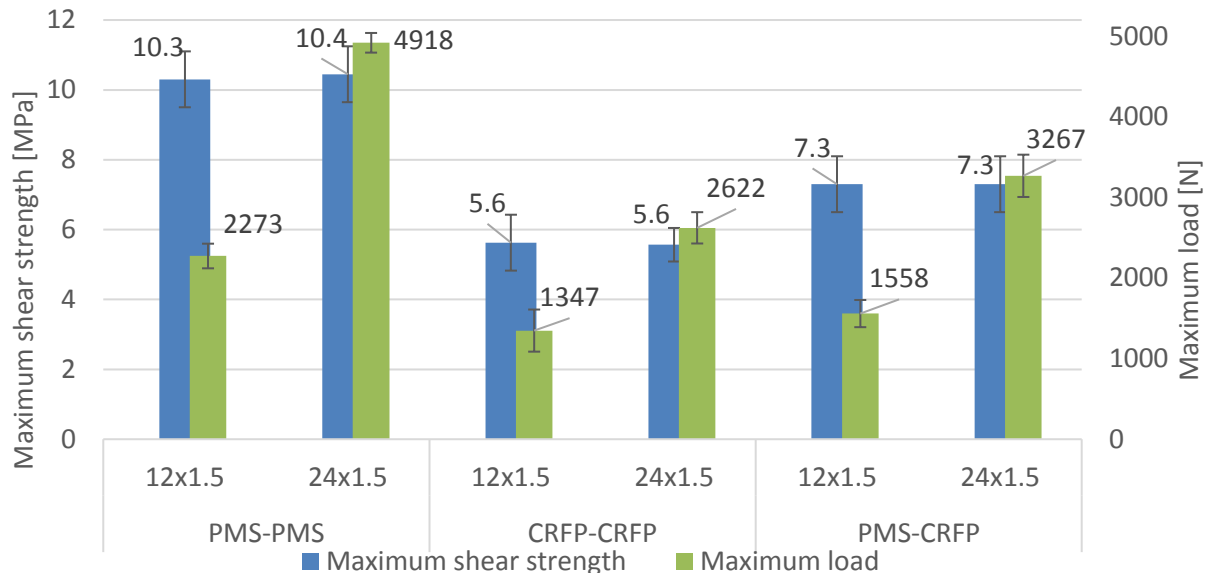

Figure 3: Summary of the result of the SLJ tests

*3.2 Correlation between experimental and numerical results*

The results of the optimization analysis are here described. Kriging method has been used to approximate the absorbed energy and the maximum force as functions of the material parameters, i.e. the maximum shear stress and the critical strain energy release rate of mode II. The optimization is executed on the approximating surfaces with the first-order algorithm COBYLA [19]. For each combination of the substrates, the optimal set of material parameters is then used to simulate the mechanical behavior of the corresponding single lap joint with 24 mm of overlap. The comparison with the corresponding experimental test finally validated the material parameters obtained with the surrogate-based optimization.
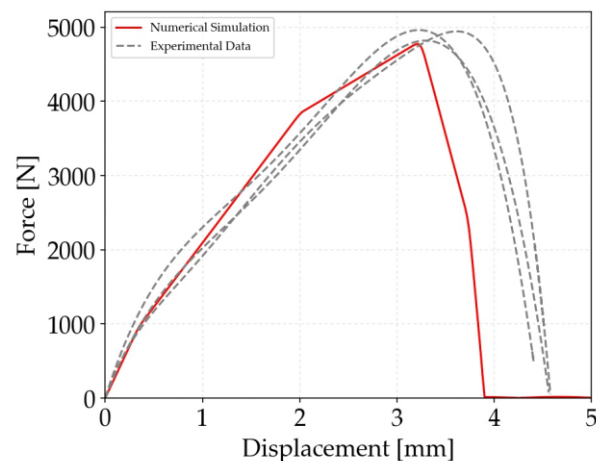
3.2.1 PMS/PMS substrates

Table 4 reports the optimal values of the shear stress and the critical strain energy release rate for the single lap joint with PMS/PMS substrates with an overlap of 12 mm, whereas in Figure 4 the numerical force-displacement curve is compared with the experimental results. The absorbed energy and the maximum force are in excellent agreement as shown in Table 4, which is also appreciable in Figure 4. The calculated optimal material parameters are then used to simulate the mechanical behavior of the PMS/PMS single lap joint with an overlap of 24 mm. Figure 5 shows the comparison of the force-displacement curve, while in Table 8 the experimental and numerical values of the absorbed energy and maximum force are reported. While the maximum force is in excellent agreement, the absorbed energy shows an error lower than 20%. This could be due to the fact that the displacement obtained experimentally is slightly larger compared to the 12 mm overlap.

Table 4. Optimal results for the PMS/PMS single lap joint with 12 mm of overlap

	Optimal results	Experimental results	Unit
S	10.0	-	MPa
G_{IIC}	23.9	-	N/mm
EN	5750	6125	J
F_{max}	2408	2408	N
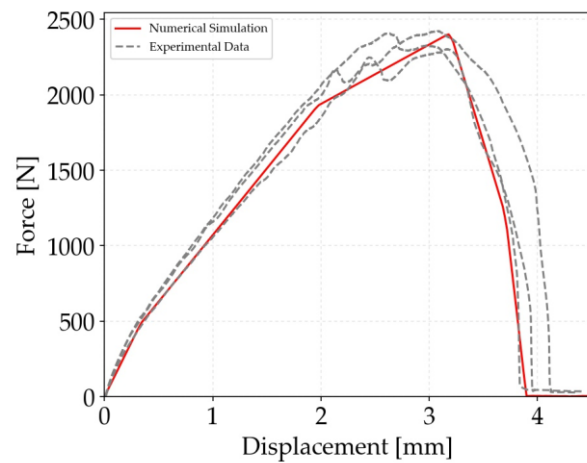
Figure 4. Comparison of the experimental and numerical force-displacement curves of the 12 mm overlap single lap joint test for the PMS/PMS configuration

Table 5. Results for the PMS/PMS single lap joint with 24 mm of overlap

	Numerical results	Experimental results	Unit
EN	11500	13980	J
F_{max}	4772	4918	N

Figure 5. Comparison of the experimental and numerical force-displacement curves of the 24 mm overlap single lap joint test for the PMS/PMS configuration

3.2.2 CFRP/CFRP substrates
Optimal values for the single lap joint with CFRP/CFRP substrates and 12 mm overlap are reported in Table 6. The comparison in terms of the force-displacement curve is shown in Figure 6. Some numerical instabilities can be appreciated after the joint has failed. However, the good agreement between the numerical and experimental results confirmed the accuracy of the surrogate model.

The calculated material parameters are then validated by comparing the numerical simulation of the single lap joint test of the 24 mm overlap with the corresponding experimental results. An excellent agreement is obtained in terms of both absorbed energy and maximum force, as reported in Table 7. Indeed, the relative error is in both cases lower than 1%, thus validating the obtained material parameters. Further, as shown in Figure 7, the force-displacement curve can reproduce the averaged trend obtained in the experimental tests.

Table 6. Optimal results for the CFRP/CFRP single lap joint with 12 mm of overlap

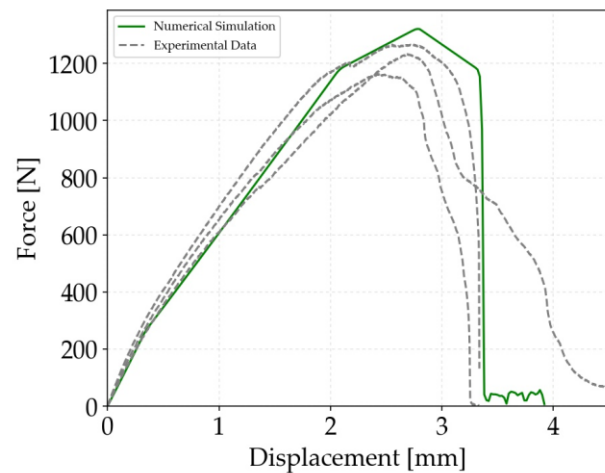|	Optimal results	Experimental results	Unit
S	5.5	-	MPa
G_{IIC}	12.0	-	N/mm
EN	2917	2924	J
F_{max}	1312	1266	N

Figure 6. Comparison of the experimental and numerical force-displacement curves of the 12 mm overlap single lap joint test for the CRFP/CRFP configuration

Table 7. Results for the CFRP/CFRP single lap joint with 24 mm of overlap

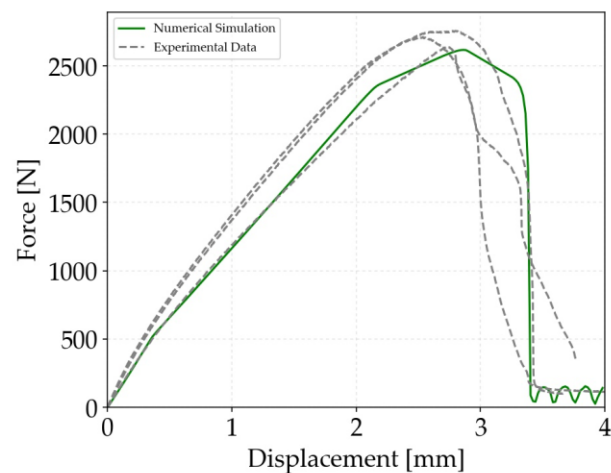|	Numerical results	Experimental results	Unit
EN	5781	5833	J
F_{max}	2616	2622	N

Figure 7. Comparison of the experimental and numerical force-displacement curves of the 24 mm overlap single lap joint test for the CRFP/CRFP configuration

3.2.3 PMS/CFRP substrates
Optimization results for the single lap joint with hybrid substrates, i.e. PMS/CFRP adherends, and 12 mm overlap are reported in Table 8, while Figure 8 compares the force-displacement curves. Even in this case, some numerical instabilities can be appreciated after the joint has failed. However, even the hybrid configuration presents a very good agreement in terms of absorbed energy and maximum force, thus confirming the accuracy of the surrogate model.

Finally, material parameters, as obtained from the surrogate-based optimization, are used to simulate the single lap joint test of the 24 mm overlap. The agreement with the corresponding experimental results is excellent both for the absorbed energy and for the maximum force, as reported in Table 9. A major relative error is obtained for the absorbed energy, which is still lower than 10%. However, as shown in

Figure 9, the force-displacement curve is in very good accordance with the experimental results, being comprised within the experimental scattering.

Table 8. Optimal results for the PMS/CFRP single lap joint with 12 mm of overlap

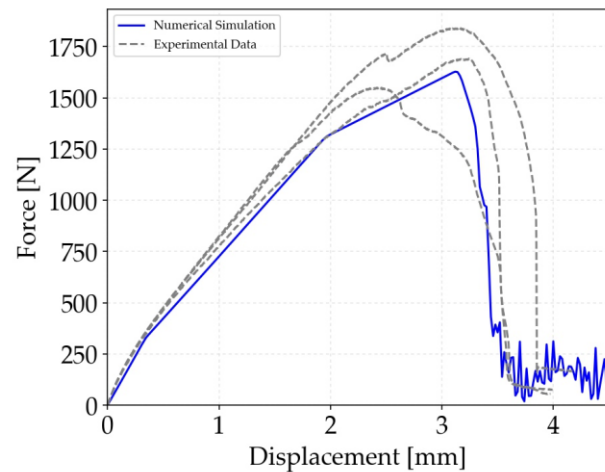|	Optimal results	Experimental results	Unit
S	6.8	-	MPa
G_{IIC}	15.75	-	N/mm
EN	3696	3700	J
F_{max}	1585	1645	N

Figure 8. Comparison of the experimental and numerical force-displacement curves of the 12 mm overlap single lap joint test for the PMS/CRFP configuration

Table 9. Results for the PMS/CFRP single lap joint with 24 mm of overlap

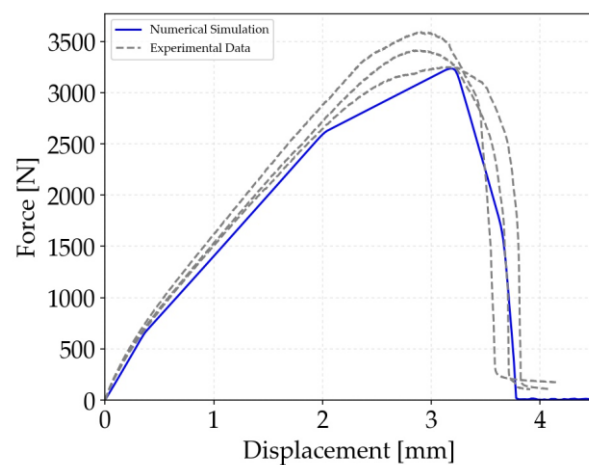|	Numerical results	Experimental results	Unit
EN	7560	8316	J
F_{max}	3236	3418	N

Figure 9. Comparison of the experimental and numerical force-displacement curves of the 24 mm overlap single lap joint test for the PMS/CRFP configuration

3.3 Fracture surfaces
Figure 10 reports the representative fracture surface of the SLJ tests for all the six analysed configurations. All the tests presented a cohesive failure that is a sign of good adhesion between the adhesive and the substrates. A sketch of a representative cohesive failure has been reported to highlight that the failure occurs within the adhesive and not between the adherend and the adhesive.
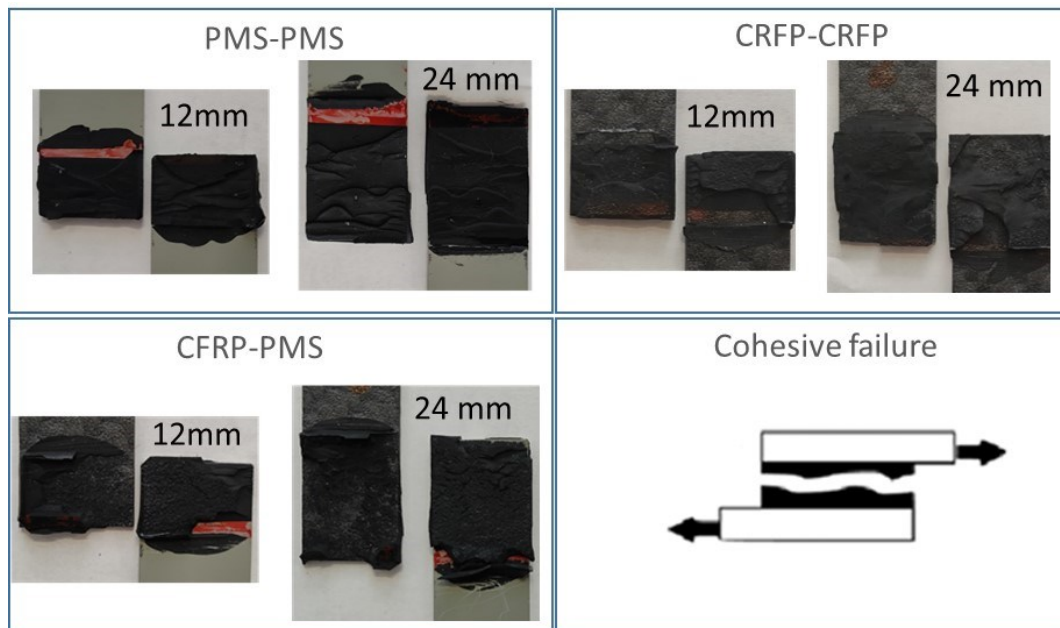
Figure 10. Representative fracture surfaces of the SLJ tests and representative cohesive failure

4. Conclusions

The work showed that polyurethane adhesive can adhesively bond PMS and CRFP substrates. The SLJ prepared with PMS-PMS substrates exhibited the maximum shear stress while the SLJ prepared with CRFP-CRFP present the lowest maximum shear strengths 45% lower compared to the PMS-PMS joints. The dissimilar SLJ present intermediate maximum shear stress, that is 29% compared to the PMS-PMS joints. The numerical simulation showed a good agreement with the experimental results.

An interesting point of the adopted approach is that it was possible to identify the required cohesive parameters simply from SLJ tests without the need for the specific fracture tests, typically DCB (Double Cantilever Beam) for mode I and ENF (End Notched Flexure) for mode II, which represents a significant advantage especially in an industrial context. Acknowledgements

Acknowledgements

References

[1]   Elmarakbi A, Ciardiello R, Tridello A, Innocente F, Martorana B, Bertocchi F, Cristiano f, Elmarakbi M, and Belingardi G 2020 Effect of graphene nanoplatelets on the impact response of a carbon fibre reinforced composite *Mater. Today Commun.* **25** p 1-11

[2]   Chang F, Scott R A and Springer G S 1984 Failure of Composite Laminates Containing Pin Loaded Holes—Method of Solution *J. Comp. Mater.* **18** p 1-26

[3]   Beyene A T Belingardi G and Koricho E G 2016 Effect of notch on quasi-static and fatigue flexural performance of Twill E-Glass/Epoxy composite *Comp. Struct.* **153** p 825-842

[4]   Chang B, Shi Y and Dong S 1999 Comparative studies on stresses in weld-bonded, spot-welded and adhesive-bonded joints. *J. Mater. Process. Technol.* **87** p 230–236

[5]   Belingardi G, and Chiandussi G 2004 Stress flow in thin-walled box beams obtained by adhesive bonding joining technology Int. *J. Adhes. Adhes.* **24** p 423–439

[6]   Lutz A Structural bonding of lightweight cars 2015 Dow Laboratory Report p 33

[7]   Banea M, and da Silva L F 2009 Adhesively bonded joints in composite materials: an overview. *Proc. IMechE Part L J. Mater.: Design Appl*. **223** p 1–18

[8]   Yi J, Boyce M C, Lee G F and Balizer F 2006 Large deformation rate-dependent stress–strain behavior of polyurea and polyurethanes *Polymer* **47**(1) p 319-329

[9]   Berntsena J F, Morina D, Clausena A and Langseth M 2019 Experimental investigation and numerical modelling of the mechanical response of a semi-structural polyurethane adhesive *Inter. J. Adhes. Adhes*. **95** p 1-12

[10] Banea M D, da Silva L F M and R D G Campilho 2015 The Effect of Adhesive Thickness on the Mechanical Behavior of a Structural Polyurethane Adhesive *J. Adhes* **91** p 331–346

[11] Saldanha D F, Cantoa S C, da Silva L F M Carbas R J, Chavesa F J P, Nomura K and Ueda T 2013 Mechanical characterization of a high elongation and high toughness epoxy adhesive *Inter. J. Adhes. Adhes*. **47** p 91-98

[12] Leal A J S, Campilho R D S G, Silva F J G, Silva D F O and Moreira F J P2019 Comparison of different test configurations for the shear fracture toughness evaluation of a ductile adhesive *Procedia Manuf*. **38** p 940–947

[13] Galvez P, Abenojar J and Martinez M A 2019 Durability of steel-CFRP structural adhesive joints with polyurethane adhesives *Compos Part B: Eng* **165** p 1-9

[14] Galvez P, Lopez de Armentia S, Abenojar J, Martinez M A 2020 Effect of moisture and temperature on thermal and mechanical properties of structural polyurethane adhesive joints *Compos. Struct*. **247** 1-13

[15] Boursier Niutta C, Ciardiello R, Belingardi G and Scattina A 2018 Experimental and numerical analysis of a pristine and a nano-modified thermoplastic adhesive PVP® *Pressure Vessels & Proc. Conf*. paper #84728.

[16] LSTC. 2019 LS-DYNA Keyword Manual Volume II

[17] Forrester A I J, Sóbester A and Keane A J 2008 Engineering Design via Surrogate Modelling: A Practical Guide, John Wiley & Sons, Ltd, Hoboken, US, p 60-100

[18] Reis P N B, Ferreira J A M and Antunes F 2011 Effect of adherend's rigidity on the shear strength of single lap adhesive joints Intern. *J. Adhes. Adhes*. **31** p 193–201

[19] Powell M J D 1994 Advances in Optimization and Numerical Analysis, Kluwer Academic, Dordrecht, NL, pp. 51-67